



Trans-oceanic transport of ^{137}Cs from the Fukushima nuclear accident and impact of hypothetical Fukushima-like events of future nuclear plants in Southern China



Ka-Ming Wai ^{a,b,*}, Peter K.N. Yu ^b

^a Department of Geological and Mining Engineering and Sciences, Michigan Technological University, Houghton, MI, USA

^b Department of Physics and Material Science, City University of Hong Kong, Hong Kong, China

HIGHLIGHTS

- A Lagrangian model was used to predict the dispersion of ^{137}Cs from plant accident.
- Observed and modeled ^{137}Cs concentrations were comparable for the Fukushima accident.
- The maximum surface concentrations could reach 10 Bq m^{-3} for the hypothetical case.
- The hypothetical radiative plumes could impact E/SE Asia and N. America.

ARTICLE INFO

Article history:

Received 20 October 2014

Received in revised form 25 November 2014

Accepted 25 November 2014

Available online xxxx

Editor: P. Kassomenos

Keywords:

Fukushima accident

Radionuclide

Long-range transport

Numerical modeling

Future impact

ABSTRACT

A Lagrangian model was adopted to assess the potential impact of ^{137}Cs released from hypothetical Fukushima-like accidents occurring on three potential nuclear power plant sites in Southern China in the near future (planned within 10 years) in four different seasons. The maximum surface ($0\text{--}500 \text{ m}$) ^{137}Cs air concentrations would be reached 10 Bq m^{-3} near the source, comparable to the Fukushima case. In January, Southeast Asian countries would be mostly affected by the radioactive plume due to the effects of winter monsoon. In April, the impact would be mainly on Southern and Northern China. Debris of radioactive plume ($\sim 1 \text{ mBq m}^{-3}$) would carry out long-range transport to North America. The area of influence would be the smallest in July due to the frequent and intense wet removal events by trough of low pressure and tropical cyclone. The maximum worst-case areas of influence were 2382000 , 2327000 , 517000 and 1395000 km^2 in January, April, July and October, respectively.

Prior to the above calculations, the model was employed to simulate the trans-oceanic transport of ^{137}Cs from the Fukushima nuclear accident. Observed and modeled ^{137}Cs concentrations were comparable. Sensitivity runs were performed to optimize the wet scavenging parameterization. The adoption of higher-resolution ($1^\circ \times 1^\circ$) meteorological fields improved the prediction. The computed large-scale plume transport pattern over the Pacific Ocean was compared with that reported in the literature.

© 2014 Elsevier B.V. All rights reserved.

1. Introduction

Extensive studies of radionuclides (e.g., ^{137}Cs , ^{133}Xe , ^{131}I) in different environmental compartments such as atmosphere, ocean and ecosystems (including animal products) were undertaken (Buesseler et al., 2011; Garnier-Laplace et al., 2011; Masson et al., 2011; Parache et al., 2011; Povinec et al., 2012) after the release of radioactive materials due to the failure of Fukushima Daiichi Nuclear Power Plant associated with the earthquake and tsunami on 11 March 2011. The atmospheric

studies included measurements at various locations in the northern hemisphere, source term estimation and transport modeling. The trans-Pacific transport of the airborne fission products such as ^{131}I and ^{137}Cs were detected in Seattle, USA, 5 to 6 d after emissions from Japan (Leon et al., 2011). In Europe, elevated concentrations of radionuclides (e.g., 1 mBq m^{-3} for ^{137}Cs and 3.6 mBq m^{-3} for ^{131}I) were measured along the Iberian Peninsula from March 28th to April 7th 2011. The pathway followed by the radioactive plume from Fukushima to there was deduced through back-trajectories analysis (Lozano et al., 2011). Eventually, the radioactive plume was carried around the globe by the westerlies in about 18 d (Hsu et al., 2012). The release rate of ^{137}Cs , which was important for atmospheric dispersion modeling, was obtained by a reverse estimation of the source term by coupling

* Corresponding author at: Department of Physics and Material Science, City University of Hong Kong, Hong Kong, China.

E-mail address: bhkmwai@cityu.edu.hk (K.-M. Wai).

environmental monitoring data with atmospheric dispersion simulations under the scenario of unit release rate (1 Bq h^{-1}). This resulted in a maximum rate of $\sim 10^{14} \text{ Bq h}^{-1}$ (Chino et al., 2011), although modification of the rate was reported (Draxler and Rolph, 2012). It is noted that a more recent estimate of emission profile for released radionuclides from the Fukushima accident was published by IRSN (http://www.irsn.fr/EN/publications/technical-publications/Documents/IRSN_Fukushima-1-year-later_2012-003.pdf). Regional and hemispheric transport behaviors of the radioactive plumes were studied by numerical models (Morino et al., 2011; Stohl et al., 2011; Draxler and Rolph, 2012). The importance and sensitivity of wet scavenging on the removal of ^{137}Cs in the modeling results were revealed (Morino et al., 2011; Draxler and Rolph, 2012).

Most of China's electricity is currently produced by fossil fuels (mostly coal) and the nuclear power generation capacity was only 1.5% of the total in 2010. However, the role of nuclear power is becoming more important, especially in coastal areas where the economy is developing rapidly. The projected contribution of nuclear power will be increased to 5% in 2020 and the contribution will grow rapidly by the end of the century [see World Nuclear Association (2012) and references therein]. Chinese regulations are to fully incorporate the safety standards of the International Atomic Energy Agency, following the Fukushima accident in March 2011. It has also been emphasized that it is highly unlikely for the planned nuclear plants in China to have serious failures such as the Fukushima one [level 7 on the INES scale (IAEA, 2011)] in view of the advanced design for new nuclear plants. For improvement on the country's emergency response capabilities and for better site selection for the plants, however, it is still beneficial to understand the potential impacts of radionuclides (e.g., ^{137}Cs) which might be released due to a plant failure in the event of an extreme disaster beyond design basis (Schnoor, 2011).

In the current study, we first explored the capability of an air pollution dispersion model in the Lagrangian framework to simulate the atmospheric transport of the radionuclide ^{137}Cs by comparing modeled data to observations made at various locations in the northern hemisphere due to the Fukushima event. The model was then used to help understand the fate of ^{137}Cs due to emissions from hypothetical plant failures in Southern China ($<30^\circ\text{N}$). Regional impact on areas where high population densities were located would be discussed.

2. Materials and methods

2.1. Simulation for hemispheric transport of Fukushima nuclear accident fallout

The transport and dispersion of ^{137}Cs radioactive plume from the Fukushima Daiichi Nuclear Power Plant was computed using the NOAA HYSPLIT4 model (Draxler and Rolph, 2013; Rolph, 2013). The HYSPLIT4 dispersion model has been used and evaluated extensively in regional and long-range transport studies (e.g. Forlano et al., 2000; Moroz et al., 2010; Stein et al., 2011; Draxler and Rolph, 2012; Chen et al., 2013). It is composed of four components: particle transport by the mean wind, a turbulent transport component, scavenging and decay, and finally the computation of the air concentration [see Draxler and Rolph (2012) and references therein for detailed description]. The model was driven by meteorological data with two different spatial resolutions. For the sensitivity runs with different sets of wet removal parameters which are discussed below, the $2.5^\circ \times 2.5^\circ$ global NCEP/NCAR reanalysis data were used because of the relatively better computational efficiency. The NCEP Global Data Assimilation System (GDAS) data with $1^\circ \times 1^\circ$ horizontal resolution was then used to simulate the hemispheric transport from the plant.

As pointed out previously that wet scavenging played an important role in computing ^{137}Cs activity concentrations, a set of model runs were performed to explore the model sensitivity to the scavenging parameters, i.e., in-cloud and below-cloud removal constants [see

Draxler and Rolph (2012) for details] and to obtain the set of best parameters when comparing with the measurements at various locations in the northern hemisphere. Four sensitivity runs with different scavenging parameters driven by meteorological fields with spatial resolution of $2.5^\circ \times 2.5^\circ$ (also known as coarse-grid model) were performed (Table 1). The best set of wet removal parameters based on the sensitivity test was adopted to simulate the Fukushima event.

A 6-hourly varied emission of ^{137}Cs from the plant was employed based on the work of Chino et al. (2011) with modifications suggested by Draxler and Rolph (2012), with the assumed release height of 100 m above ground, which compromised between the low-level and more thermal/explosive emissions. In search for a better emission profile, we also tested the IRSN profile described above by making additional model runs with all other model settings kept identical to those described here. We found, however, that the modeling results predicted by the IRSN profile were 2–3 orders of magnitude larger than the observed concentrations at the measurement stations. Since the model performance using the IRSN profile was not better than that using our adopted profile, we did not use the IRSN profile here. The atmospheric release of ^{137}Cs for our simulation here started on 11 March 2011 and ended 24 d after. The concentration grid was global with $1^\circ \times 1^\circ$ resolution with the surface layer from 0 to 500 m. In the Lagrangian framework, the concentration was calculated by summing the mass of all the particles as they passed over a concentration grid. The concentration grid was user-defined by the grid dimensions which were independent of the meteorological grid. A particle diameter of $1 \mu\text{m}$ was assumed although there was large variability in the diameter of particulate radionuclides [see Morino et al. (2011) and reference therein]. Radioactive decay of ^{137}Cs (half-life = 30.2 y), as well as wet and dry removal were included in the model. A three-dimensional particle approach by releasing 30,000 particles for each release time period was set in the model. The settings were the same as those adopted by Draxler and Rolph (2012).

Surface-level (1.5 m above ground) ^{137}Cs measurements at Anaheim (California) in USA (U.S. Environmental Protection Agency's radiological sampling network – RADNET, <http://www.epa.gov/japan2011/rert/radnet-sampling-data.html>), Sidney (BC) in Canada (Zhang et al., 2011) and Sacavem (Lisbon) in Portugal (Carvalho, 2012) were used for model evaluation. These sites were distant from the source and the data were suitable for testing the model performance of long-range transport of ^{137}Cs .

2.2. Simulation for radioactive plume transport for hypothetical Fukushima-like accidents

The same HYSPLIT4 Lagrangian dispersion model described previously was used. The model was driven by the NCEP Global Data Assimilation System (GDAS) data with the $1^\circ \times 1^\circ$ horizontal resolution. The patterns of radioactive plume for the four seasons (in January, April, July and October) were simulated to obtain more representative modeling results. The total simulation period was 20 d from the beginning of the month so that the patterns of radioactive plume in terms of both initial and long-range transport could be investigated. To put the plant locations in different provinces along the coast of Southern China ($<30^\circ\text{N}$) into more realistic perspectives, information on the planned plants provided by the World Nuclear Association (2012) was employed. These

Table 1
Wet removal constants used for the sensitivity test.

Scenario	In-cloud (l/l)	Below-cloud (s^{-1})
S1 ^a	4×10^4	5×10^{-6}
S2	4×10^4	5×10^{-7}
S3	4×10^3	5×10^{-6}
S4	4×10^5	5×10^{-6}

^a Values in S1 were used by Draxler and Rolph (2012).

plants were located in the Guangdong Province (GD: 22.6° N, 114.6° E), Fujian Province (Fu: 25.4° N, 119.5° E) and Zhejiang Province (Zh: 29.1° N, 121.6° E). We used the identical emission profile adopted for our Fukushima event to simulate the hypothetical events. This approach has been used to study hypothetical events in the USA (Ten Hoeve and Jacobson, 2012). The accuracy of the modeled results was highly dependent on the adopted source term, the knowledge on which could be improved by inverse modeling and ensemble simulations. However, as a preliminary assessment here, application of these approaches was beyond the scope of the present paper. We have done sensitivity model runs and found that the uncertainties of source term and the resulted modeled concentrations were the same. All other model settings were the same as those described previously.

3. Results and discussion

3.1. Sensitivity runs and model evaluation

The computed concentrations at the three sites were found to be more sensitive to the in-cloud wet removal constant (Table 1). When the in-cloud removal constant was reduced (increased), significant over-estimation (under-estimation) of the computed values related to the observations occurred for scenario S3 (S4). For example, the median ratio of modeled/observed values at Sidney (BC), Canada was 22 ($n = 9$) for S3, compared to 0.5 ($n = 9$) for S2. In-cloud scavenging for S4 was too large so that the computed concentrations at the three sites were too low ($< 10^{-5} \text{ mBq m}^{-3}$ for most cases) compared to the observations. Compared to the in-cloud removal constant, the modification of the below-cloud constant was relatively insensitive to the computed results. Overall speaking, there was little improvement in the computed concentrations for S2 compared with S1 in relation to the observations, and thus the constants for S2 were adopted for all further simulations as discussed below.

The Lagrangian model was then driven by meteorological fields with both lower (coarse-grid model) and higher spatial resolution of $1^\circ \times 1^\circ$ (also known as fine-grid model), to investigate if its performance was improved for the fine-grid model. The computed and observed concentrations at the three sites are presented in Fig. 1. For the site Anaheim (California) in the USA, the observed concentration on 18 March 2011 was not simulated. However, no ^{137}Cs -rich air was measured but it was simulated on 19 March 2011. The radioactive plume was not captured until 20 March by the fine-grid model. It was noted that the coarse-grid model only captured the plume on 25 March, although agreement between the computed and observed concentration on the day was even better than that obtained using the fine-grid model. For the site Sidney (BC) in Canada, the coarse-grid model captured the plume 2 d before the fine-grid one on 23 March 2011. However, it failed to capture the plume on 29 March, 1 and 2 April 2011. When the radioactive plume was transported further east and over the Atlantic Ocean, it hit Portugal which was the forefront country in the European continent. The fine-grid model captured the plume with a comparable concentration on 27 March 2011 although it failed to do so for the previous day. The coarse-grid model was able to capture the plume only until 2 April 2011. It demonstrated that reproduction of the plume transport behavior could be improved by adopting a higher resolution meteorological dataset.

The computed surface-level ^{137}Cs concentrations were also compared with the modeling results from Ten Hoeve and Jacobson (hereafter referred to as Te12) (Ten Hoeve and Jacobson, 2012). On 14 March 2011, both studies showed that the plume reached the longitude 170° E (with plume center around 40° N) with comparable computed concentrations of $0.5\text{--}1 \text{ mBq m}^{-3}$. On 20 March 2011, a tongue of high concentrations (in the order of 10^2 mBq m^{-3}) extended eastward. A branch of the plume moved southward ($\sim 1 \text{ mBq m}^{-3}$) and another branch moved anti-cyclonically towards eastern Siberia (Fig. 2). Both models predicted the pattern although the branches of the plume predicted

by Te12 moved closer to Philippine and more inland of Siberia. The eastward-going plume reached inland of North America with some radioactive debris even over the Atlantic Ocean. Our model computed an area of higher concentrations (with a maximum of 1 mBq m^{-3}) located over the Eastern Pacific Ocean within 20–30° N, compared to a bigger extent of the plume towards high latitudes computed by Te12. On 26 March 2011, both models found the ^{137}Cs signature in air nearly for the entire northern hemisphere.

3.2. Potential impact of ^{137}Cs released from hypothetical accidents

The model was used to forecast releases from hypothetical accidents in nuclear power plants in Southern China. The radioactive plume transport would be mainly affected by the East Asian monsoon. In winter months under the influence of the winter monsoon, southwestward transport of the radioactive plume released from the plants would affect the coastal provinces in Southern China. When the plume was transported further south/southwestward, it would affect Southeast Asian countries such as Vietnam, Laos, Thailand, the Philippines, Malaysia and Indonesia. The ^{137}Cs activity concentrations over the Southeast Asian countries would be relatively high due to the insignificant wet removal of the radioactive plume by the dry air mass. In summer months the radioactive plume would be transported north/northeastward by the air mass associated with the summer monsoon, in such a way that the coastal provinces in northern China ($> 30^\circ \text{ N}$), as well as Korea and Japan would be affected. The associated rainfall with unstable air of the monsoon would lead to a significant wet removal of the radioactive plume. Therefore, lower ^{137}Cs concentrations would be predicted over these areas. Table 2 shows the worst-case area of influence (AOI, km^2) experienced with activity concentrations of ^{137}Cs larger than 10 mBq m^{-3} from the radioactive plume released from the potential plant sites.

3.2.1. Radioactive plume transport in January

Fig. 3 shows the evolution of the radioactive plume of ^{137}Cs from the three potential plant sites (i.e., GD, Fu and Zh) in January. For the GD case, the radioactive plume would be mainly transported southwestward once the ^{137}Cs laden plume was emitted. Since the plant would be located near the coast, inland areas of the Southern China with large populations would not suffer from significant impact over the first 2 d (except Hong Kong, Fig. 3a). The plume would then continue its southwest transport and spread more eastward following the continental outflow. After 8 d, South-east Asia countries such as Vietnam, Laos, Thailand, Malaysia and northern Philippines, as well as Taiwan and more inland areas of Southern China, would be affected by the plume. The AOI with activity concentrations of 100 mBq m^{-3} was 368000 m^2 . The maximum activity concentration was predicted to reach 10 Bq m^{-3} around the source, which was comparable to the CMAQ model results for the Fukushima event (Morino et al., 2011). The value was also comparable to the maximum observed value at Takasaki, Japan [250 km from the Fukushima Dai-chi nuclear power plant, see Schöppner et al. (2012) and references therein]. After 13 d, the radioactive plume would be further transported southward and Indonesia also experienced its impact. Near the source, southern Vietnam and Malaysia would experience elevated concentrations in the order of 100 mBq m^{-3} . After 20 d, the plume would continue its east-west spread near the equator and be dissipated due to the heavy rainfall at the Inter-tropical Convergence Zone (ITCZ). The plume with elevated concentrations would be mainly located over the oceanic areas such as the Indian Ocean/Bay of Bengal.

For the Fu and Zh plant sites, the evolution of radioactive plume would be similar to that for the GD case except for the following. The eastward advection of the plume to the Western Pacific Ocean would be pronounced in such a way that Taiwan had a higher impact especially for the Zh case. For instance, Taiwan would suffer the plume impact in the order of 100 mBq m^{-3} after 9–13 d of release from the Zh site. In

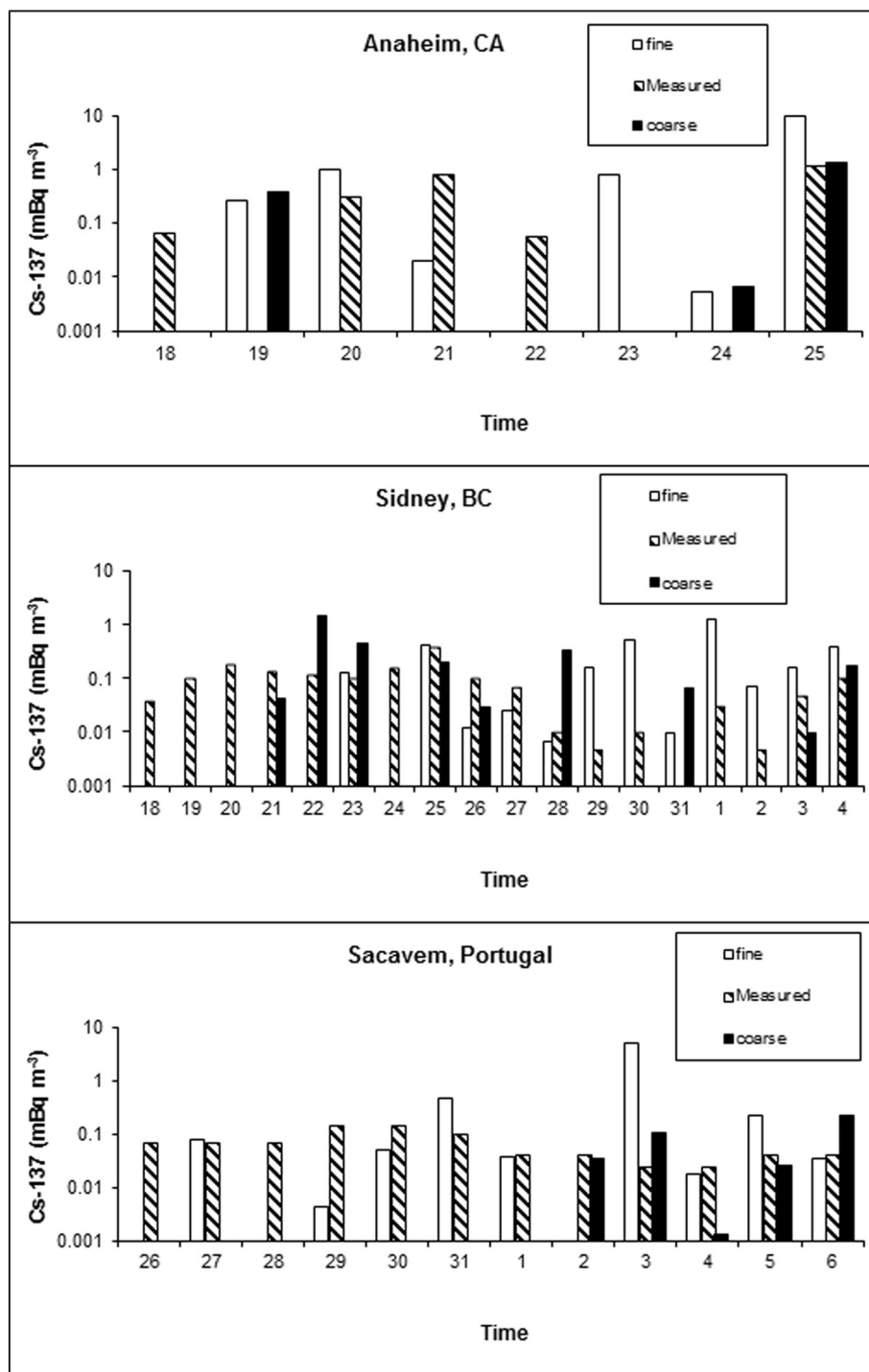


Fig. 1. Computed and observed ^{137}Cs concentrations (mBq m^{-3}) at the three sites. X-axis shows the days starting from March. Coarse = coarse-grid model; Fine = fine-grid model.

addition, South-east Asian countries would suffer less impact (with concentrations lower by one order of magnitude) from the Zh plant after 10 d of release.

3.2.2. Radioactive plume transport in April

The winter monsoon would be weakened in April so the transport would be smaller than that in January for all the plant locations after 2 d of release (Supplementary material S1a). For the GD case, there would be a southwestward transport of the radioactive plume due to a weak continental outflow after 4 d. However, the outflow would then be replaced by a maritime flow with reversed wind direction. The combined effects would be that after 8 d, more inland area of

Southern China would be suffered from the plume impact (Supplementary material S1a). The total populated area having experienced elevated concentrations in the order of 1 Bq m^{-3} was 144000 m^2 . On the other hand, the impact on the South-east Asian countries would be minimal ($\leq 1 \text{ mBq m}^{-3}$). An area with concentrations in the order of 1 Bq m^{-3} would then be prevalent to the north of the source. After 13 d, the plume would spread further north ($> 30^\circ \text{ N}$). Another plume component would be transported to east/southeast to the Philippines and the Western Pacific. The plume with concentrations of 1 Bq m^{-3} would be located to the north of the source and Taiwan. The area with elevated concentrations would then tend to move eastward over the oceanic area and would be dissipated by wet removal associated with a trough

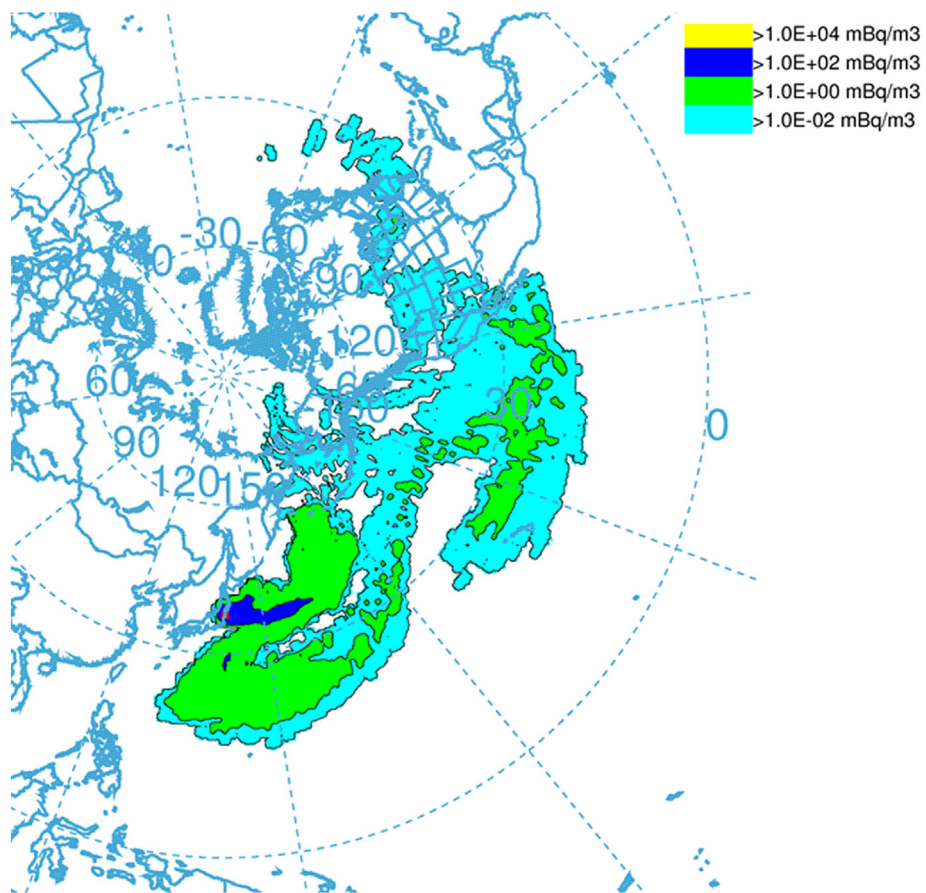


Fig. 2. Computed ^{137}Cs concentrations (mBq m^{-3}) by Hysplit4 model on 20 March (polar-map projected).

of low pressure. These would result in a reduction in the impact of the radioactive plume on populated areas after 20 d of release (Supplementary material S1a). In addition, debris of radioactive plume ($\sim 1 \text{ mBq m}^{-3}$) could experience long-range transport to the North America over the Pacific Ocean.

For releases from the Fu and Zh plant sites, the evolution of the radioactive plume would be similar to that for the GD case except for the following. For the Fu case, the plume with concentrations 1 Bq m^{-3} would be located to the west/southwest of the source (Supplementary material S1b). For the Zh case, there would be a component of the plume dispersing northward, which would then move eastward to affect South Korea and southern Japan after 8 d (Supplementary material S1c). Another wave of radioactive plume dispersion would undergo in a similar way after 13 d of release, leading to elevated concentrations of 100 mBq m^{-3} over South Korea and southern Japan two days later. The plume would then be dissipated by wet removal which was evident by low pressure systems there (surface pressure map not shown).

3.2.3. Radioactive plume transport in July

The summer monsoon was featured with unstable southerly/southwesterly airstream. Therefore, coastal Provinces in northern China, Korea and Japan would experience the impact of the radioactive plume. For the GD case after 2 d, the plume impact would be mainly on the coastal area of northern China (Fig. 4). The plume would then affect South Korea and southern Japan. It was noted, however, that the plume would not spread widely as the cases in January and April. The impact on South Korea and southern Japan would also be relatively small ($\leq 10 \text{ mBq m}^{-3}$) after 8 d. The plume strength would then be dissipated quickly by heavy rainfall associated with board areas of low pressure, tough and tropical cyclone over East Asia and the Western Pacific. This would result in the smallest AOI among the four seasons with concentrations larger than 10 mBq m^{-3} .

For releases from the Fu and Zh plants, the evolution of the radioactive plume (Fig. 4) would be similar to that for the GD case except for the following. The arrival of the radioactive plume to South Korea and Japan would be within 2 d. The countries would experience higher concentrations ($\sim 100 \text{ mBq m}^{-3}$) especially for the Zh case but the impact would be transient ($< 2 \text{ d}$ out of the first 8 d of release). The northmost impacted area would be at near 60° N but with very small concentrations ($\sim 0.1 \text{ mBq m}^{-3}$). Again the Fu and Zh cases would have the smallest AOI among the four seasons.

3.2.4. Radioactive plume transport in October

The effects of winter monsoon became important again, although the monsoon was not strong as that in January as discussed above. Meanwhile, wet removal events by the trough of low pressure and rain-band associated with typical cyclone would reduce the radioactive plume impact. For the GD case, there would be a southwest transport of

Table 2
Worst-case area of influence (km^2) where ^{137}Cs concentrations $> 10 \text{ mBq m}^{-3}$.

Season	Plant		
	GD	Fu	Zh
January	2,382,000	900,000	529,000
April	1,517,000	2,327,000	2,125,000
July	517,000	163,000	151,000
October	1,321,000	1,312,000	1,395,000

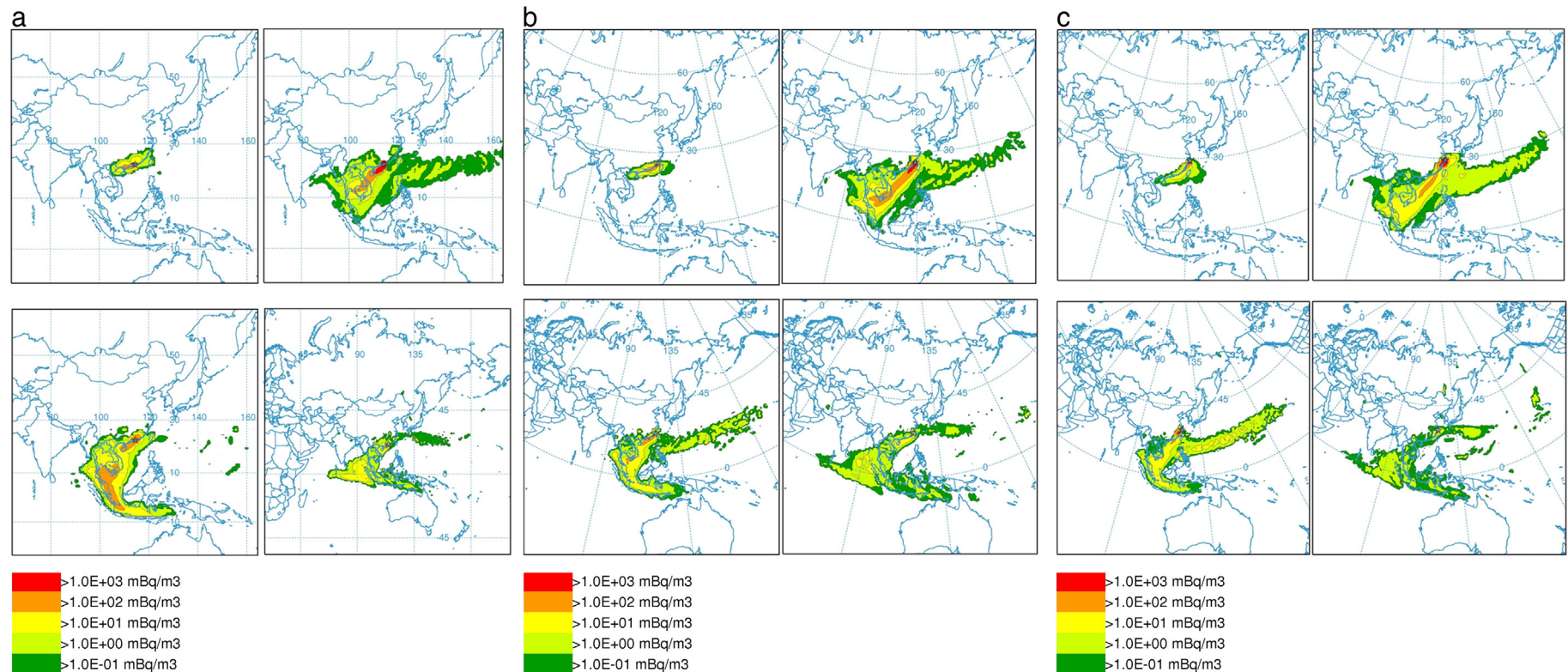


Fig. 3. Evolution of surface-level ^{137}Cs activity concentrations (mBq m^{-3}) of the radioactive plume 2 d (upper left), 8 d (upper right), 13 d (lower left) and 20 d (lower right) after the initial release from the hypothetical (a) GD; (b) Fu; and (c) Zh plant location in January.

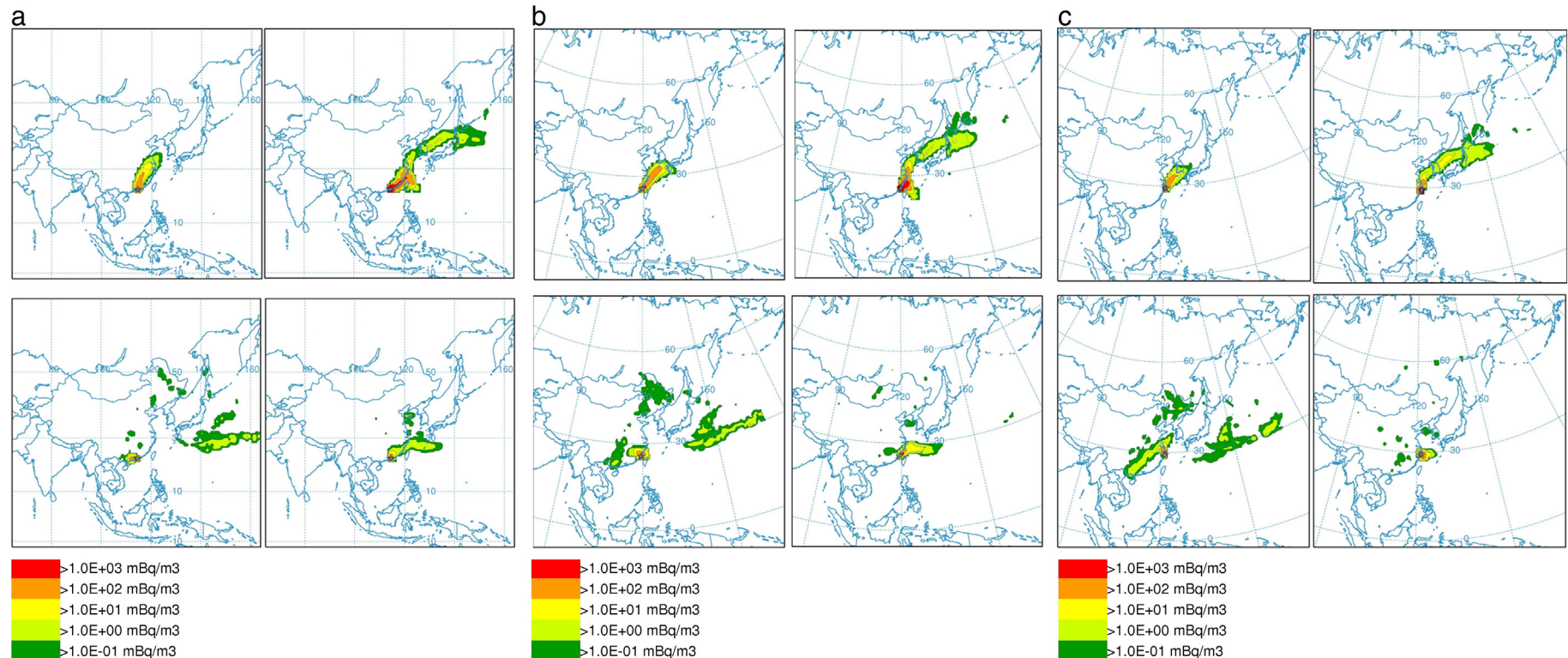


Fig. 4. Evolution of surface-level ^{137}Cs activity concentrations (mBq m^{-3}) of the radioactive plume 2 d (upper left), 8 d (upper right), 13 d (lower left) and 20 d (lower right) after the initial release from the hypothetical (a) GD; (b) Fu; and (c) Zh plant location in July.

the plume along the coast line of Southern China after 2 d of release, due to the combined effects of the winter monsoon and the tropical cyclone at the South China Sea (Supplementary material S2a). The plume would then affect Southeast Asian countries. Within the first 8 d from the release, the evolution of the plume transport would be similar to the January case but the impact for the October case would be smaller due to the wet removal by the rain-band associated with the typical cyclone. Following the dissipation of the tropical cyclone at the South China Sea, the impact of the radioactive plume on Southeast Asian countries would become larger after 8 d of release (Supplementary material S2a). However, the wet removal associated with the low pressure centered at the South China Sea would prevent the growth of ^{137}Cs concentrations over Southeast Asia countries, especially over the coastal areas. This would result in a smaller AOI over there after 13 d, when compared to the January case. After 20 d, Southeast Asia countries at lower latitudes ($<10^\circ \text{ N}$) would not experience a noticeable impact from the plume, due to the weaker airflow and previous wet removal events.

For the Fu plant site release, the evolution of radioactive plume would be similar to that for the GD case (Supplementary material S2b). For the Zh case, the plume evolution would be similar to the GD case within the first 7 d after the release only. After 8 d, the radioactive plume would be transported inland of China following the on-shore flow. There would be two plume components – one would move southwestward as for the GD and Fu cases and another would move northward (Supplementary material S2c). After 13 d, the southwest-going component would transport more inland and the resulted AOI would be larger than those for the GD and Fu cases. The evolution of the plume component and the impact on Southeast Asian countries would then be similar to those for the GD and Fu cases until the end of simulation. For the north-going component, the impacted area would extend to the latitude of 40° N . The component would tend to move eastward and affect Korea and Japan with lower concentrations ($<1 \text{ mBq m}^{-3}$), and would then be dissipated after 20 d.

4. Conclusions

Using an identical emission profile to Fukushima, hypothetical Fukushima-like cases occurring on potential nuclear plant sites in Southern China were simulated for four different seasons. In January, the GD plant release would lead to the largest worst-case AOI ($2,382,000 \text{ km}^2$) with ^{137}Cs concentrations larger than 10 mBq m^{-3} during the 20 d simulation using year 2011 meteorology (same year of the Fukushima accident). The impacted areas would be mainly in Southeast Asian countries such as Vietnam, Laos, Cambodia, Thailand, the Philippines, Malaysia and Indonesia, as well as a small part of the coastal areas of Southern China. In April, the impact would occur frequently in the coastal areas and inland of both southern and northern China (but not Southeast Asia countries), so the worst-case AOI would be generally large ($>1,500,000 \text{ km}^2$) for all the potential cases. This was due to the on-shore flow when the winter monsoon was weakened. The impact could occur at higher latitudes over South Korea and southern Japan for the Zh plant release. July would be in a season with the smallest worst-case AOI ($<550,000 \text{ km}^2$) among all potential plant sites. This was due to the southwesterly flow associated with the summer monsoon, frequent wet removal events associated with the trough of low pressure and the tropical cyclone, and the location of the plants. A larger worst-case AOI would be obtained for the GD plant since the radioactive plume would affect Southern China, small areas in northern China and South Korea. The location of the Fu and Zh plants would lead to a reduction in the impact on Southern China. Relatively complex flow patterns in October were found, in such a way that the worst-case AOI would be located very differently for the GD/Fu and Zh cases. For the former plant, Southeast Asian countries ($>10^\circ \text{ N}$) and part of Southern China would be impacted by the radioactive plume. For the latter,

both Southern and Northern China would be impacted. Nevertheless, the worst-case area of influence would be similar for all the plant sites ($1,300,000\text{--}1,400,000 \text{ km}^2$).

Acknowledgment

The authors gratefully acknowledge the NOAA Air Resources Laboratory (ARL) for the provision of the HYSPLIT transport and dispersion model and/or READY website (<http://ready.arl.noaa.gov>) used in this publication.

Appendix A. Supplementary data

Supplementary data to this article can be found online at <http://dx.doi.org/10.1016/j.scitotenv.2014.11.084>.

References

- Buesseler K, Aoyama M, Fukasawa M. Impacts of the Fukushima Nuclear Power Plants on marine radioactivity source. *Environ. Sci. Technol.* 2011;45:9931–5.
- Carvalho FP. Radioactivity from Fukushima nuclear accident detected in Lisbon, Portugal. *J. Environ. Radioact.* 2012;114:152–6.
- Chen B, et al. Size distribution and concentrations of heavy metals in atmospheric aerosols originating from industrial emissions as predicted by the HYSPLIT model. *Atmos. Environ.* 2013;71:234–44.
- Chino M, et al. Preliminary estimation of release amounts of ^{131}I and ^{137}Cs accidentally discharged from the Fukushima Daiichi nuclear power plant into the atmosphere. *J. Nucl. Sci. Technol.* 2011;48:1129–34.
- Draxler RR, Ralph GD. Evaluation of the Transfer Coefficient Matrix (TCM) approach to model the atmospheric radionuclide air concentrations from Fukushima. *J. Geophys. Res.* 2012;117:D05107.
- Draxler RR, Ralph GD. HYSPLIT (HYbrid Single-Particle Lagrangian Integrated Trajectory) Model access via NOAA ARL READY Website. Silver Spring, MD: NOAA Air Resources Laboratory; 2013 (<http://ready.arl.noaa.gov/HYSPLIT.php>).
- Forlano L, Hedgecock IM, Pirrone N. Elemental gas phase atmospheric mercury as it interacts with the ambient aerosol and its subsequent speciation and deposition. *Sci. Total Environ.* 2000;259:211–22.
- Garnier-Laplace J, Beugelin-Seiller K, Hinton TG. Fukushima wildlife does reconstruction signals ecological consequences. *Environ. Sci. Technol.* 2011;45:5077–8.
- Hsu SC, et al. Hemispheric dispersion of radioactive plume laced with fission nuclides from the Fukushima nuclear event. *Geophys. Res. Lett.* 2012;39:L00G22.
- IAEA. Briefing on Fukushima Nuclear Accident. www.iaea.org/newscenter/news/tsunamiupdate01.html, 2011.
- Leon DJ, et al. Arrival time and magnitude of airborne fission products from the Fukushima, Japan, reactor incident as measured in Seattle, WA, USA. *J. Environ. Radioact.* 2011;102:1032–8.
- Lozano RL, et al. Radioactive impact of Fukushima accident on the Iberian Peninsula: evolution and plume previous pathway. *Environ. Int.* 2011;37:1259–64.
- Masson O, et al. Tracking of airborne radionuclides from the damaged Fukushima Dai-Ichi Nuclear Reactors by European Networks Source. *Environ. Sci. Technol.* 2011;45:7670–7.
- Morino Y, Ohara T, Nishizawa M. Atmospheric behavior, deposition, and budget of radioactive materials from the Fukushima Daiichi nuclear power plant in March 2011. *Geophys. Res. Lett.* 2011;38:L00G11.
- Moroz BE, et al. Predictions of dispersion and deposition of fallout from nuclear testing using the NOAA-HYSPLIT meteorological model. *Health Phys.* 2010;99:252–69.
- Parache V, et al. Transfer of I-131 from Fukushima to the vegetation and milk in France source. *Environ. Sci. Technol.* 2011;45:9998–10003.
- Povinec PP, Hirose K, Aoyama M. Radio-strontium in the Western North Pacific: characteristics, behavior, and the Fukushima impact source. *Environ. Sci. Technol.* 2012;46:10356–63.
- Rolph GD. Real-time Environmental Applications and Display sYstem (READY) Website. Silver Spring, MD: NOAA Air Resources Laboratory; 2013 (<http://ready.arl.noaa.gov>).
- Schnoor JL. Lessons from Fukushima source. *Environ. Sci. Technol.* 2011;45:3820.
- Schöppner M, et al. Estimation of the time-dependent radioactive source-term from the Fukushima nuclear power plant accident using atmospheric transport modelling. *J. Environ. Radioact.* 2012;114:10–4.
- Stein AF, et al. Modeling PM10 originating from dust intrusions in the Southern Iberian Peninsula Using HYSPLIT. *Weather Forecast.* 2011;26:236–42.
- Stohl A, et al. Xenon-133 and caesium-137 releases into the atmosphere from the Fukushima Dai-ichi nuclear power plant: determination of the source term, atmospheric dispersion, and deposition. *Atmos. Chem. Phys. Discuss.* 2011;11:28319–94.
- Ten Hoeve JE, Jacobson MZ. Worldwide health effects of the Fukushima Daiichi nuclear accident. *Energy Environ. Sci.* 2012;5:8743–57.
- World Nuclear Association. <http://www.world-nuclear.org/info/inf63.html>, 2012.
- Zhang W, et al. Development of a new aerosol monitoring system and its application in Fukushima nuclear accident related aerosol radioactivity measurement at the CTBT radionuclide station in Sidney of Canada. *J. Environ. Radioact.* 2011;102:1065–9.